

# **Discrete Modeling of Solute Transport in a Homogeneous Porous Medium**

S Semmar, N Bendjaballah-Lalaoui

Department of Chemical Engineering, University of Science and Technology Houari Boumediene (USTHB) , Algeria

**Abstract:** This work presents the study of one-dimensional and unidirectional transport of non-reactive solute through a saturated and homogeneous porous medium in a laboratory column. Based on the discrete approach, two models were discussed. The first called classical model (CM) established when local thermodynamic equilibria are reached; however, the second was the mobile/immobile model (MIM). This model takes into account the physical non-equilibrium (PNE), so the pore space is divided into “mobile” and “immobile” flow regions with first-order mass transfer between these two regions. The objective of this work is the determination of the analytical solution of the transport equation for both models using Inverse Laplace transforms based on the method of residues. Validation of each equation is made through a calculation code that we developed in MATLAB to optimize the experimental breakthrough curves (BTCs). The results obtained show that for a moderate flow rate ( $Q= 5\text{ml/min}$ ) the BTCs present an asymmetry, the assumption of physical equilibrium on which the CM model based, is sometimes inadequate. This justified the application of the MIM model.

**Keywords:** Modeling, Analytical solution, Solute transport, Physical non equilibrium, Porous media.

## Nomenclature

BTC	breakthrough curve.
CDE	convection dispersion equation.
CM	classical model.
MIM	mobile-immobile model.
PNE	physical non equilibrium.
C	concentration of solute in contact with an aggregate [M L <sup>-3</sup> ].
C <sup>-</sup>	Laplace transforms of C.
D <sub>0</sub>	molecular diffusion coefficient in free water [L <sup>2</sup> T <sup>-1</sup> ].
d	diameter of column [L].
dp	diameter of a soil particle [L].
F(t)	function of the BTC from step inputs.
G(s)	global transfer function for the column.
G(T)	transfer function in time domain.
g <sub>k</sub> (s)	transfer function for cell k.
J	number of mixing cells.
K <sub>im</sub>	ratio of immobile water fraction to mobile water fraction
k <sub>M</sub>	mass transfer coefficient [T <sup>-1</sup> ].
L	length of column [L].
M	mass of the porous medium [M].
N	number of observation concentration data.
Q	volumetric flow rate [L <sup>3</sup> T <sup>-1</sup> ].
R <sup>2</sup>	correlation coefficient.
Sp	area of a soil particle [L <sup>2</sup> ].
s	Laplace transform parameter.
t <sub>M</sub>	characteristic mass transfer time [T].

# International Journal of Innovative Research in Science, Engineering and Technology

(An ISO 3297: 2007 Certified Organization)

Vol. 5, Issue 11, November 2016

$t$	the time [T].
$t_m$	characteristic convective time[T].
$V$	volume of the medium [L <sup>3</sup> ].
$V_p$	volume of a soil particle [L <sup>3</sup> ].
$v_m$	Darcy velocity [LT <sup>-1</sup> ].
$y_i$	observed concentrations.
$\hat{y}_i$	simulated concentrations.
$\varepsilon$	external porosity.
$\theta$	volumetric water content.
$\theta_m, \theta_{im}$	volume fraction of mobile and immobile water relative to the whole volume.
$\rho_l$	fluid density [M L <sup>-3</sup> ].
$\mu_k$	kth order time moment [T <sup>k</sup> ].
$\sigma^2$	variance of BTC [T <sup>2</sup> ].
$\sigma'^2$	reduced variance.
$\delta$	thick of the thin film surrounding the particle [L].
$\eta_e$	dynamic viscosity of water [ML <sup>-1</sup> T <sup>-1</sup> ].

## I. INTRODUCTION

The study of the transport of solute in a saturated porous media has received increasing attention in different fields, such as hydrogeology, petroleum engineering, (soil) hydrology, and waste disposal sites construction. For instance, aquifer systems are often vulnerable to contaminants and need special protection when used as sources for drinking water [1].

The hypothesis that has been used widely in solute transport to reduce its complexity is that the medium properties are invariant and local equilibrium assumption is valid during the transport [2-7]. In the field conditions at a given velocity, these assumptions sustain an ideal transport behavior. However, there are many macro and micro level processes which influence the applicability of ideal transport. Practically the equilibrium assumption does not exist in the real field conditions and the nature of the solute transport is always in non-equilibrium regime. The PNE transport of contaminant is reported in the literature [8-13].

Generally, the behavior of the solute transport through porous medium is represented by BTCs. The shape of BTCs can be used to understand the transport behavior [14].

Sudicky et al [10] and Starr et al [11] observed the behavior of BTCs from the elution of non-reactive and reactive solute through stratified porous medium. The nature of BTCs showed a significant departure from classical dispersion–diffusion theory. It was found that there are some interactions influencing the transport of contaminant which is not explained by classical theory. The distribution of BTCs resulting from the elution of solute through porous medium under the influence of non-equilibrium condition is asymmetrical.

The PNE will affect transport because of nonuniformity of the flow field at the pore scale including preferential and unstable flow [15-17]. The mobile/immobile model has commonly been used to account for PNE during solute transport [18, 19]. In this case, the pore space is partitioned into two regions. Transport in the “mobile” region of the pore space is described with the convection–dispersion equation (CDE) while solute exchange between “mobile” and “immobile” regions occurs by diffusion and is typically described with a first-order rate equation. The mobile/immobile model predicts early initial BTC as a result of rapid transport through the “mobile” region, and extended tailing of the BTC as a result of slow diffusion between the “immobile” to the “mobile” region.

Less research has been undertaken to examine the effect of the pore water velocity on movement of the solute. Yan Li Jiang et al [20] study the influences of different pore water velocities on solute transport through undisturbed loessial soil columns collected from the Loess Plateau, chloride BTCs generated by pulse inputs were fitted by both the

# International Journal of Innovative Research in Science, Engineering and Technology

(An ISO 3297: 2007 Certified Organization)

Vol. 5, Issue 11, November 2016

convection dispersion equation (CDE) and MIM model. The effects were also reflected in the model parameters of each model. Both models fitted the experimental data, although the MIM model tended to fit the data better than the CDE especially for high pore water velocity. An analysis of the model parameters showed that, when pore water velocity increased, the mobile-immobile partition coefficient tended to decrease and the mass transfer coefficient tended to increase.

A large number of specialized models now exist to simulate the various processes at various levels and for different applications [21]. Modeling approaches range from relatively simple analytical and semianalytical solutions, to much more complex numerical codes that permit consideration of a large number of simultaneous nonlinear processes.

The use of numerical models is now also very much facilitated by the availability of specific software packages in both the public and commercial domains, including the development of sophisticated graphical user interfaces that dramatically simplify their use [22, 23]. Examples of widely used codes for flow and transport in variably saturated or multiphase systems are MACRO [24], UNSATCHEM [25], FEHM [26], HYDROBIOGEOCHEM [27], VS2DI [28], MODFLOW-SURFACT [29], STOMP [30], SWAP [31], and the HYDRUS [32] and TOUGH [33] family of codes.

While semi-analytical and analytical solutions undoubtedly remain popular for many applications. Neville et al [34] and Semra et al [35] proposed a semianalytical approach. After applying a Laplace transform of the governing equations for the PNE model, the solute concentration was obtained by numerical inversion.

Currently, analytical solutions can typically only be obtained for linear transport problems for simplified conditions, such as well-defined conditions in laboratory experiments. However analytical methods are also useful to verify numerical methods, elucidate the role of different model parameters, and to quantify approximately the transport such as for longer time or spatial scales [36]. It should also be noted that detailed numerical simulations are often not warranted because of a lack of reliable model parameters. Therefore analytical solution for the MIM model will still be valuable.

This article presents the modeling of non-reactive solute transport through a saturated and homogeneous porous medium in a laboratory column. Our focus is especially on transport processes in Laboratory scale experiments. First we give a brief overview of the classical solute transport equations, which used for modeling equilibrium solute transport processes in saturated media. Next we provide a brief discussion of possible PNE transport formulations often needed for flow processes in porous media

The principal objective of this work is to derive analytical solution for the MIM model that offers the flexibility to quantify the impact of PNE solute transport processes in laboratory soil columns. A secondary objective of this work is to apply the new solution of the MIM model to describe BTCs reported by Semra et al [35].

## II. DISCRETE APPROACH

The discrete approach or the mixing-cell-in series model expresses the convective-dispersive solute through porous media as a constant flow rate through a finite number,  $J$ , of identical mixing cells or agitated reactors. A mixing cell size is equal to  $V/J$  (Fig.1). It is generally expressed in term of length,  $L/J$ , where  $L$  is the whole medium length. It is equivalent to an aggregation of a few grains and the surrounding fluid [37].

# International Journal of Innovative Research in Science, Engineering and Technology

(An ISO 3297: 2007 Certified Organization)

Vol. 5, Issue 11, November 2016

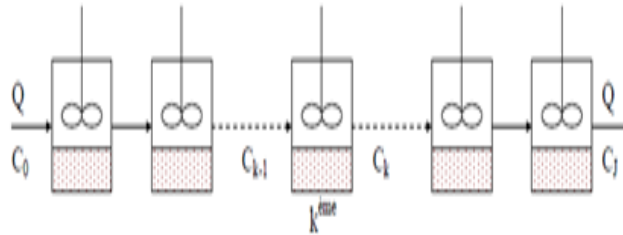


**Fig.1:** Discrete approach to represent solute transport into porous media

### Classical model (CM)

This model considers that the local thermodynamic equilibria are established. The solute transport is obtained from mass balance in one cell which rank is  $k$  (Fig 2), [38].

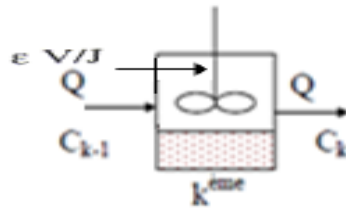


**Fig.2:** Classical model of solute transport

$$QC_{k-1} = QC_k + \frac{d(C_k V')}{dt}$$

$$QC_{k-1} = QC_k + \frac{d(C_k V')}{dt} \tag{1}$$

$$QC_{k-1} = QC_k + \epsilon \frac{V}{J} \frac{dC_k}{dt} \tag{2}$$

Where  $C_{k-1}$  and  $C_k$  are cell  $k$  inlet and outlet fluid-in-flow concentrations respectively [ $N/L^3$ ];  $Q$ , the constant flow rate [ $L^3/T$ ];  $V$  the medium global volume [ $L^3$ ];  $\epsilon$  the external porosity.

### The mobile/immobile model (MIM)

This model has commonly been used to account the PNE during solute transport. In this case, the liquid is distributed between the mobile zone and the immobile zone (Fig.3). The exchange of solute between these two regions obeys a linear law [39].

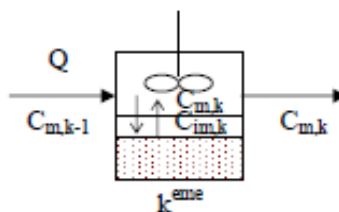


**Fig.3:** Mobile/immobile model of solute transport

## International Journal of Innovative Research in Science, Engineering and Technology

(An ISO 3297: 2007 Certified Organization)

Vol. 5, Issue 11, November 2016

The two governing equations for solute transport in a porous medium with mobile and immobile regions of soil water are defined as:

$$Q C_{m,k-1} = Q C_{m,k} + \frac{\theta_m V}{J} \frac{dC_{m,k}}{dt} + \frac{k_{MV}}{J} (C_{m,k} - C_{im,k-1}) \quad (3)$$

$$\frac{k_{MV}}{J} (C_{m,k} - C_{im,k-1}) = \frac{\theta_{im} V}{J} \frac{dC_{im,k}}{dt} \quad (4)$$

where  $Q$  is the constant flow rate [ $L^3/T$ ],  $\theta$  is the volumetric water content, the subscripts  $m$  and  $im$  refer to the mobile and immobile region,  $C_k$  is the concentration of the aqueous phase in the mixer  $k$  [ $N/L^3$ ],  $V$  the medium global volume [ $L^3$ ], and  $k_M$  is a PNE coefficient for mass transfer between mobile and immobile region [ $1/T$ ].

### III. DERIVATION OF THE ANALYTICAL SOLUTION

#### Solution for CM Model

Taking the Laplace transform of the governing equation (equation (2)), one has:

$$Q \overline{C_{k-1}} = Q \overline{C_k} + \varepsilon \frac{V}{J} s \overline{C_k} = Q \overline{C_k} \left[ 1 + \frac{\varepsilon V}{J Q} s \right] \quad (5)$$

Where  $s$  denotes the Laplace transform parameter;  $\overline{C_{k-1}}$  and  $\overline{C_k}$  represents the Laplace transforms of  $C_{k-1}$  and  $C_k$ , respectively.

From equation (5), transfer function for cell  $k$ ,  $g_k(s)$ , relating respective inlet and outlet fluid concentration Laplace transforms is written according to equation (6).

$$g_k(s) = \frac{\overline{C_k}}{\overline{C_{k-1}}} = \left[ 1 + \frac{t_m}{J} s \right]^{-1} \quad (6)$$

Where  $t_m$  is the characteristic convective time through the medium, it is calculated by:

$$t_m = \frac{\varepsilon V}{Q} \quad (7)$$

However, the  $J$  ordinary differential equations (2) are replaced by  $J$  algebraic equations (5). Each algebraic equation represents a unique cell transfer function. Finally, the global transfer function for the column,  $G(s)$ , is given by:

$$G(s) = \frac{\overline{C_J}}{\overline{C_0}} = \left[ 1 + \frac{t_m}{J} s \right]^{-J} = \left( \frac{a}{a+s} \right)^J \quad (8)$$

Where

$$a = \frac{J}{t_m} \quad (9)$$

So, the model (CM) is then a model with a single parameter, which is the number of mixers,  $J$ .

The above solutions are derived in the Laplace domain. To obtain the time domain solutions,  $G(T)$ , the Laplace solutions must be inverted. One can easily obtain the inverse Laplace transform of  $G(s)$ .

The solution in real-time domain is as follows:

$$G(t) = \frac{a^J t^{J-1} \exp(-a t)}{(J-1)!} \quad (10)$$

The response curves from **step inputs** is the function  $F(t)$  called the breakthrough curve. The function  $F(t)$  can be obtained by integrating .

$$F(t) = \int_0^t G(t) dt \quad (11)$$

In these case  $F(t)$  is given by:

$$F(t) = -\frac{\exp(-a t)}{(J-1)!} \times \sum_{n=1}^J \frac{(J-1)!}{(J-n)!} \times (at)^{J-n} \quad (12)$$

# International Journal of Innovative Research in Science, Engineering and Technology

(An ISO 3297: 2007 Certified Organization)

Vol. 5, Issue 11, November 2016

## Solution for MIM Model

With the Laplace transform of Eq. (3) and Eq. (4), one can obtain:

$$Q\overline{C_{m,k-1}} = Q\overline{C_{m,k}} + \frac{\theta_m V}{J} s\overline{C_{m,k}} + \frac{k_M V}{J} (\overline{C_{m,k}} - \overline{C_{im,k}}) \quad (13)$$

$$\frac{\theta_{im} V}{J} s\overline{C_{im,k}} = \frac{k_M V}{J} (\overline{C_{m,k}} - \overline{C_{im,k}}) \quad (14)$$

Where  $s$  denotes the Laplace transform parameter;  $\overline{C_{m,k-1}}$ ,  $\overline{C_{m,k}}$  and  $\overline{C_{im,k}}$  represent the Laplace transforms of  $C_{m,k-1}$ ,  $C_{m,k}$ ,  $C_{im,k}$ , respectively and  $\theta_m$ ,  $\theta_{im}$  represent the volume fraction of mobile and immobile water relative to the whole volume.

One finds from equations (13-14):

$$Q\overline{C_{m,k-1}} = Q\overline{C_{m,k}} + \frac{\theta_m V}{J} s\overline{C_{m,k}} + \frac{\theta_{im} V}{J} s\overline{C_{im,k}} \quad (15)$$

So, stage  $k$  transfer function is:

$$g_k(s) = \frac{\overline{C_{m,k}}}{\overline{C_{m,k-1}}} = \left[ 1 + \frac{t_m}{J} s(1 + M(s)) \right]^{-1} \quad (16)$$

Where:

$t_m = \frac{\theta_m V}{Q}$  is the characteristic convective time.

$K_{im} = \frac{\theta_{im}}{\theta_m}$  is the ratio of immobile water fraction to mobile water fraction.

$t_M = \frac{\theta_{im}}{k_M}$  is the characteristic mass transfer time.

$$M(s) = \frac{K_{im}}{1 + t_M s} \quad (17)$$

The global transfer function for the column,  $G(s)$ , is given by:

$$G(s) = \frac{\overline{C_J}}{\overline{C_0}} = \left[ 1 + \frac{t_m}{J} s(1 + M(s)) \right]^{-J} = \left( \frac{a}{a + s(1 + \frac{b}{c+s})} \right)^J \quad (18)$$

With:  $a = \frac{J}{t_m}$ ,  $b = \frac{K_{im}}{t_M}$ ,  $c = \frac{1}{t_M}$

So, the model MIM is then a model with three parameters, which are the number of mixers,  $J$ , the mobile fraction,  $\theta_m$  and mass transfer coefficient  $K_M$ .

## Analytical inversion of the solutions in the Laplace domain

Given the complexity of the Eq. (18), it is not easy to obtain a simple closed-form expression for solute concentration through analytical inverse Laplace transform. Generally, the Laplace solutions were inverted numerically to derive semi-analytical solution.

There are several numerical Laplace inversion methods such as the Stehfest [40], Crump [41] and de Hoog et al [42] methods, among others. These models used the Fourier series in the inversion formula, they has been widely applied in numerous flow and transport problems [43, 34, 35, 44, 45].

Therefore, using analytical solution here is as best as we can get from a semi-analytical perspective. The analytical solution offers a convenient way to explore solute transport behavior, its accuracy has been substantially proven and it may provide benchmarks for the testing of more general numerical models. The Cauchy's Residue Theorem [47] is used here to calculate the concentration in real-time domain.

# International Journal of Innovative Research in Science, Engineering and Technology

(An ISO 3297: 2007 Certified Organization)

Vol. 5, Issue 11, November 2016

## Cauchy's Residue Theorem

If C is a simple closed, positively oriented contour in the complex plane and f is analytic except for some points  $z_1, z_2, \dots, z_n$  inside the contour C, then

$$\frac{1}{2\pi i} \int_C f(z) dz = \sum_{k=1}^n \text{Res } f(z_k) \quad (19)$$

If f has a pole of order k at  $z = z_0$  then

$$\text{Res } f(z_0) = \frac{1}{(k-1)!} \lim_{z \rightarrow z_0} \frac{d^k}{dz^k} \{(z - z_0)^k f(z)\} \quad (20)$$

## The Inverse Laplace Transform

Given G(s), we can calculate G(t) using the Bromwich inversion formula

$$G(t) = \frac{1}{2\pi i} \int_{\gamma - i\infty}^{\gamma + i\infty} G(s) e^{st} ds \quad (21)$$

Here  $\gamma$  is a real constant, and the Bromwich inversion contour  $\tau$  run from  $\gamma - i\infty$  to  $\gamma + i\infty$  along a straight line.

$\tau$  must lie to the right of all the singularities of G(s)

By the residue theorem, where  $s_1, s_2, \dots, s_n$  are the poles of G(s), we deduce that

$$G(t) = \sum_{k=1}^n \text{Res}_{s=s_k} (G(s) e^{st}) \quad (22)$$

## The solution in real-time domain

The decomposition in simple elements gives:

$$G(s) = \frac{a^{(c+s)^J}}{(s+A)(s+B)^J} \quad (23)$$

$$A = \frac{(a+b+c) - \sqrt{(a+b+c)^2 - 4ac}}{2} \quad (24)$$

$$B = \frac{(a+b+c) + \sqrt{(a+b+c)^2 - 4ac}}{2} \quad (25)$$

$$G(s) = \frac{a^J (c+s)^J}{(s+A)^J (s+B)^J} \quad (26)$$

From equation (17), G (s) is a rational function of the form:

$$G(s) = \frac{P(s)}{Q(s)} \quad (27)$$

The roots of P (s) = 0 is the zero of the function G (s).

The roots of Q (s) = 0 are the poles of G (s), because G (s) tends to infinity for these points.

So, the poles of G(s) are (-A) and (-B)

Using the equations (21) and (23):

$$G(t) = \text{Res}(-A) + \text{Res}(-B) \quad (28)$$

Using the equation (22):

$$\text{Res}(-A) = \frac{1}{(J-1)!} \left[ \frac{d^{J-1}}{ds^{J-1}} (s+A)^J \frac{a^J (c+s)^J}{(s+A)^J (s+B)^J} e^{st} \right]_{s=-A} \quad (29)$$

$$= \frac{a^J}{(J-1)!} \left[ \frac{d^{J-1}}{ds^{J-1}} \frac{(c+s)^J}{(s+B)^J} e^{st} \right]_{s=-A} \quad (30)$$

Apply the general **Leibniz rule** to calculate the derivative of the equation (30):

$$(\mathbf{f} \cdot \mathbf{g})^{(n)}(\mathbf{x}) = \sum_{k=0}^n \mathbf{C}_n^k \mathbf{f}^{(k)}(\mathbf{x}) \mathbf{g}^{(n-k)}(\mathbf{x}) \quad (31)$$

## International Journal of Innovative Research in Science, Engineering and Technology

(An ISO 3297: 2007 Certified Organization)

Vol. 5, Issue 11, November 2016

$$\left(\frac{(c+s)^J}{(s+B)^J} e^{st}\right)^{(J-1)} = \sum_{k=0}^{J-1} C_{J-1}^k \left(\frac{(c+s)^J}{(s+B)^J}\right)^{(k)} (e^{st})^{(J-k-1)} \quad (32)$$

$$\left(\frac{(c+s)^J}{(s+B)^J}\right)^{(k)} = \sum_{p=0}^k C_k^p \left(\frac{1}{(s+B)^J}\right)^{(p)} ((c+s)^J)^{(k-p)} \quad (33)$$

One finds from equations (32-33):

$$\text{Res}(-A) = \frac{a^J}{(J-1)!} \left[ \sum_{k=0}^{J-1} C_{J-1}^k \left( \sum_{p=0}^k C_k^p \left(\frac{1}{(s+B)^J}\right)^{(p)} ((c+s)^J)^{(k-p)} \right) (e^{st})^{(J-k-1)} \right]_{s=-A} \quad (34)$$

Or:

$$\left(\frac{1}{(s+B)^J}\right)^{(p)} = (-1)^p \frac{(J+p-1)!}{(J-1)! (s+B)^{J+p}} \quad (35)$$

$$((c+s)^J)^{(k-p)} = \frac{J!}{(J-(k-p))!} (c+s)^{J-(k-p)} \quad (36)$$

$$(e^{st})^{(J-k-1)} = t^{(J-k-1)} (e^{st}) \quad (37)$$

Then:

$$\text{Res}(-A) = \frac{a^J}{(J-1)!} \left[ \sum_{k=0}^{J-1} C_{J-1}^k \left( \sum_{p=0}^k C_k^p (-1)^p \frac{(J+p-1)!}{(J-1)!} \frac{1}{(s+B)^{J+p}} \frac{J!}{(J-(k-p))!} (c+s)^{J-(k-p)} \right) t^{(J-k-1)} (e^{st}) \right]_{s=-A} \quad (38)$$

$$\text{Res}(-A) = \frac{Ja^J}{(J-1)!} \sum_{k=0}^{J-1} C_{J-1}^k \sum_{p=0}^k C_k^p (-1)^p \frac{(J+p-1)!}{(J-(k-p))!} \frac{(c-A)^{J-(k-p)}}{(B-A)^{J+p}} t^{J-k-1} e^{-At} \quad (39)$$

By analogy Res(-B) can be written:

$$\text{Res}(-B) = \frac{Ja^J}{(J-1)!} \sum_{k=0}^{J-1} C_{J-1}^k \sum_{p=0}^k C_k^p (-1)^p \frac{(J+p-1)!}{(J-(k-p))!} \frac{(c-B)^{J-(k-p)}}{(A-B)^{J+p}} t^{J-k-1} e^{-Bt} \quad (40)$$

The function G (t) is as follows:

$$G(t) = \frac{Ja^J}{(J-1)!} \sum_{k=0}^{J-1} C_{J-1}^k \sum_{p=0}^k C_k^p (-1)^p \frac{(J+p-1)!}{(J-(k-p))!} \frac{(c-A)^{J-(k-p)}}{(B-A)^{J+p}} t^{J-k-1} e^{-At} \\ + \frac{Ja^J}{(J-1)!} \sum_{k=0}^{J-1} C_{J-1}^k \sum_{p=0}^k C_k^p (-1)^p \frac{(J+p-1)!}{(J-(k-p))!} \frac{(c-B)^{J-(k-p)}}{(A-B)^{J+p}} t^{J-k-1} e^{-Bt} \quad (41)$$

Or:

$$F(t) = \int_0^t G(t) dt \quad (42)$$

So :

$$\int_0^t t^{J-k-1} e^{-At} dt = \frac{(J-k-1)!}{A^{J-k}} - \sum_{r=1}^{J-k} \frac{(J-k-1)!}{(J-k-r)!} \frac{t^{J-k-r}}{A^r} e^{-At} \quad (43)$$

Then, the function F(t) is given by:

$$F(t) = \frac{Ja^J}{(J-1)!} \sum_{k=0}^{J-1} C_{J-1}^k \sum_{p=0}^k C_k^p (-1)^p \frac{(J+p-1)!}{(J-(k-p))!} \frac{(c-A)^{J-(k-p)}}{(B-A)^{J+p}} \left[ \frac{(J-k-1)!}{A^{J-k}} - \sum_{r=1}^{J-k} \frac{(J-k-1)!}{(J-k-r)!} \frac{t^{J-k-r}}{A^r} e^{-At} \right] + \\ \frac{Ja^J}{(J-1)!} \sum_{k=0}^{J-1} C_{J-1}^k \sum_{p=0}^k C_k^p (-1)^p \frac{(J+p-1)!}{(J-(k-p))!} \frac{(c-B)^{J-(k-p)}}{(A-B)^{J+p}} \left[ \frac{(J-k-1)!}{B^{J-k}} - \sum_{r=1}^{J-k} \frac{(J-k-1)!}{(J-k-r)!} \frac{t^{J-k-r}}{B^r} e^{-Bt} \right] \quad (44)$$

#### IV. THE BREAKTHROUGH CURVE MOMENTS

Moment analysis of the BTC constitutes a more general approach to characterize solute transport in porous media.

# International Journal of Innovative Research in Science, Engineering and Technology

(An ISO 3297: 2007 Certified Organization)

Vol. 5, Issue 11, November 2016

## Theoretical moments

Theoretical, the breakthrough curve moments can be determined from the global transfer function  $G(s)$  according to Van Der Laan relation (equation (45)) without any need to inverse  $G(s)$  [48]:

$$\mu_k = (-1)^k \left. \frac{\partial^k G(s)}{\partial s^k} \right|_{s=0} \quad (45)$$

$\mu_k$  is the  $k^{\text{th}}$  order time moment.

One of the most important moments is the first order one,  $\mu_1$

Calculation of the second order moment,  $\mu_2$  allows calculation of the variance  $\sigma^2$  and, consequently, the reduced variance  $\sigma'^2$ .

The variance is:

$$\sigma^2 = \mu_2 - \mu_1^2 \quad (46)$$

Hence :

$$\sigma'^2 = \frac{\sigma^2}{\mu_1^2} \quad (47)$$

## Breakthrough moments for CM:

$$\mu_1 = t_m \quad (48)$$

$$\sigma'^2 = \frac{1}{J} \quad (49)$$

The reduced variance of CM model is function of hydrodynamics dispersion only.

## Breakthrough moments for MIM:

$$\mu_1 = t_m(1 + M(0)) = t_m(1 + K_{im}) \quad (50)$$

$$\frac{1}{J} + \frac{2K_{im} t_m}{(1+K_{im}) \mu_1} \quad (51)$$

$$\sigma'^2 = \frac{1}{J} - \frac{2M'(0)}{\mu_1(1+M(0))} =$$

In this case the reduced variance is composed in two terms: the first one is related only to the hydrodynamic dispersion  $1/J$ , and the second term is related to mass transfer kinetics ( $M'(0)$ ). It shows that hydrodynamics and exchange effects are separated and are only added to each other.

## Experimental moments

As with any statistical distribution, moments for a residence time distribution (RTD) is defined by:

$$\mu_1 = \int_0^{\infty} (1 - F(t)) dt \quad (52)$$

$$\sigma^2 = \int_0^{\infty} 2t(1 - F(t)) dt - \mu_1^2 \quad (53)$$

$$\sigma'^2 = \frac{\sigma^2}{\mu_1^2} \quad (54)$$

The calculation of experimental moments was making by using the *trapezoidal rule* programmed in MATLAB.

Exemplar based inpainting technique is used for inpainting of text regions, which takes structure synthesis and texture synthesis together. The inpainting is done in such a manner, that it fills the damaged region or holes in an image, with surrounding colour and texture. The algorithm is based on patch based filling procedure. First find target region using mask image and then find boundary of target region. For all the boundary points it defined patch and find the priority of these patches. It starts filling the target region from the highest priority patch by finding the best match patch. This procedure is repeated until entire target region is inpainted.

# International Journal of Innovative Research in Science, Engineering and Technology

(An ISO 3297: 2007 Certified Organization)

Vol. 5, Issue 11, November 2016

The algorithm automatically generates mask image without user interaction that contains only text regions to be inpainted.

## V. ANALYTICAL SOLUTION VALIDATIONS

### The calculation code used for the modeling of solute transport

The calculation code that we developed, based on the Method of Least Squares, use the solution of the transport equations obtained for the two models to fit experimental breakthrough curves (BTCs) at different flows rate.

The BTCs were simultaneously fitted with the analytical solution of CM and MIM model. With the above, we determined each model parameters, then we calculated theoretical reduced variances and we compared to the experimental ones.

The various parameters intervening in the calculation are: the number of mixers J, residence time (for CM), more then, the fraction of mobile water  $\theta_m$  and the mass transfer coefficient  $k_M$  (for MIM). The optimization of one or more of these parameters can also be performed using the method of least squares.  $\theta_m$  varies from  $0.5\varepsilon$  to  $\varepsilon$ , and the interval of  $k_M$  is calculate by the relation given by [49] :

$$k_M = \frac{D_0}{\delta} \cdot \frac{S_p}{V_p} \cdot \frac{\theta_{im}}{\theta} \quad (55)$$

Where:

$S_p$  and  $V_p$  are respectively the area and volume of a soil particle with diameter  $d_p$ , in the case of spherical particles,  $V_p / S_p = d_p / 6$ ,  $\delta$  is the thick of the thin film surrounding the particle and  $D_0$  is the molecular diffusion coefficient in free water.

To calculate  $\delta$ , Chen et al [50] used the relationship of Wilson and Geankopolis, 1966:

$$\frac{D_0}{\delta} = 1.09 v_m \left( \frac{\rho_l d_p \theta v_m}{\eta_e} \right)^{-\frac{2}{3}} \left( \frac{\eta_e}{\rho_l D_0} \right)^{-\frac{2}{3}} \quad (56)$$

Where  $\eta_e$  is the dynamic viscosity of water [ $ML^{-1}T^{-1}$ ],  $\rho_l$  is the fluid density [ $M L^{-3}$ ],  $v_m$  is the Darcy velocity [ $LT^{-1}$ ] and  $\theta$  is the volumetric water content.

The determination coefficient ( $R^2$ ) was used as a criteria to reflect the goodness of the fitting, which can be expressed as:

$$R^2 = 1 - \frac{\sum_{i=1}^N (y_i - \hat{y}_i)^2}{\sum_{i=1}^N (y_i - \bar{y})^2} \quad (57)$$

Where  $y_i$  and  $\hat{y}_i$  are the observed and simulated concentrations respectively, N is the number of observation concentration data at a specific flow rate.

### Experimental validation of models

The BTCs used to validate the models are realized by Semra [35]. It is about a series of experiment on laboratory column for three flow rates 1, 2 and 5ml/min (Table 1).

column	d(cm)	L(cm)	M(g)	V <sub>p</sub> (ml)	$\varepsilon$
Chromo1	1	6.4	1.52	4.2	0.83

**Table1:** Geometrical and operational parameters

# International Journal of Innovative Research in Science, Engineering and Technology

(An ISO 3297: 2007 Certified Organization)

Vol. 5, Issue 11, November 2016

## VI. RESULTS AND DISCUSSIONS

### Application of CM model to the experimental results

The figure 4 illustrates an example of the fitted of the BTC experimental by CM model at a flow rate of 1ml/min.

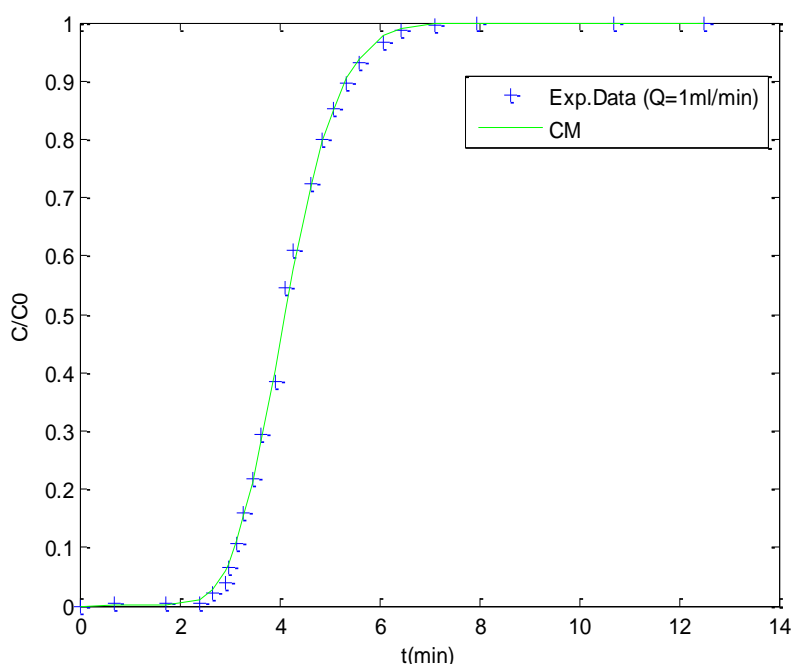


**Fig.4:** Example of the fitted of the BTC experimental (Exp. Data) by the CM model.

We note a good agreement between the CM model and the experimental BTC.

We have gathered in the following table all the results obtained for various flows rates.

Flow rate (ml/min)	1	2	5
$J_{opt}$	23	23	12
$R^2_{CM}$	0.9989	0.9988	0.9986
$\sigma'^2_{exp}$	0.0456	0.0511	0.1116
$\sigma'^2_{theor}$	0.0435	0.0435	0.0833

**Table 2:** CM model validation.

The CM model provides that the variance reduced in a medium is constant  $\sigma'^2 = \frac{1}{J}$  (J is constant); it does not depend on the flow rate.

We noted that the value of J optimized is constant and equal to 23 for the low flow rates (1 and 2 ml/min), which proves the validity of the choice of the CM model of transport. However, the fitting at a flow rate of 5 ml/min is done for a J different from 23, and equal to 12, in this case the flow rate has an effect on the variance which does not correspond to the CM model. Therefore, we conclude that for a rather large flow rate, a more complex model will be adapted better than the CM model.

## International Journal of Innovative Research in Science, Engineering and Technology

(An ISO 3297: 2007 Certified Organization)

Vol. 5, Issue 11, November 2016

According to Tevissen [51], the variation of the variance with the flow rate can be explained by the presence of an immobile fraction of water which exchanges a solute with the mobile fraction, and in this case the flow rate affects the reduced variance according to the following relations.

$$\sigma'^2 = \sigma_0'^2 + kQ \tag{58}$$

This relation is in the same as the relation of the reduced variance obtained by experimental method:

$$\sigma'^2 = 0.0281 + 0.0107Q \quad \text{With } R^2 = 0.9432 \tag{59}$$

### Application of MIM model to the experimental results

The figure 5 represents the fitted of the BTC by MIM model at a flow rate of 5 ml/min.

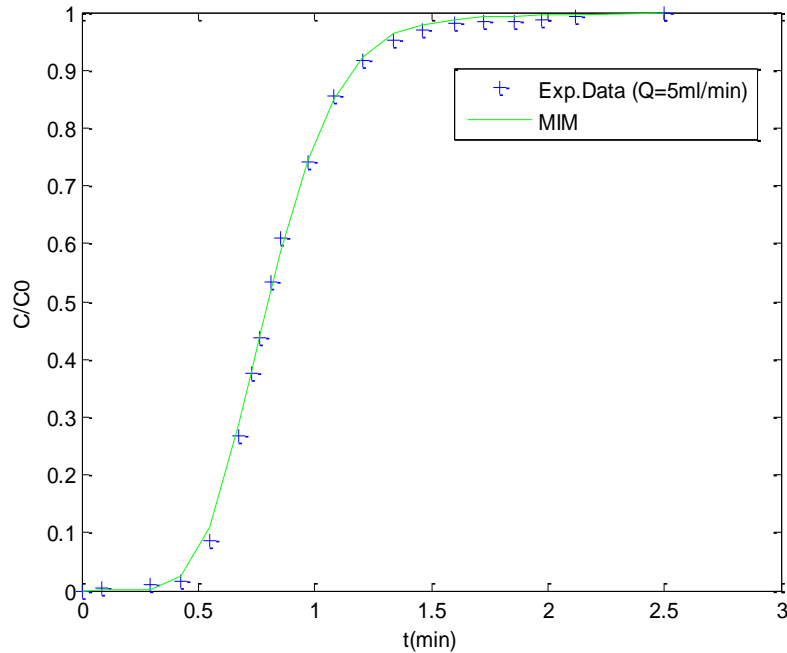


**Fig.5:** Fitted of the BTC (Exp. Data) for 5ml/min by MIM model.

We note a good agreement between the MIM model and the experimental curve.

We have gathered in the following table all the results obtained for the three flows rates.

Flow rate (ml/min)	1	2	5
J	23	23	12
R <sup>2</sup>	0.9979	0.9951	0.9992
$\theta_m$	0.829	0.829	0.816
$k_m$	0.013	0.025	0.028
$\sigma'^2_{exp}$	0.0456	0.0511	0.1116
$\sigma'^2_{theor}$	0.0435	0.0435	0.1036

**Table 3:** MIM model validation.

## International Journal of Innovative Research in Science, Engineering and Technology

(An ISO 3297: 2007 Certified Organization)

Vol. 5, Issue 11, November 2016

For the two flow rates 1 and 2 ml / min, the fitting shows that MIM model tends to CM model. This is confirmed by the negligible values of  $\theta_{im} = 0.001$  and the identical values of the variances  $\sigma'^2_{theor\ MIM} = \sigma'^2_{theor\ CM} = 1/j$ . However, for the flow rate 5 ml / min, the immobile fraction exists  $\theta_{im} = 0.014$  and theoretical variance value is closed to the experimental value. This explains that the MIM model fits the experimental curve better than the CM model.

### Effect of the flow rate on BTC

In order to study the effect of the flow rate on the solute transport, the fitted BTCs are represented at the three flow rates on function of time based on the first order moment of each BTC. Then, the fitted parameters of the CM and of MIM models are examined (Tab.4).

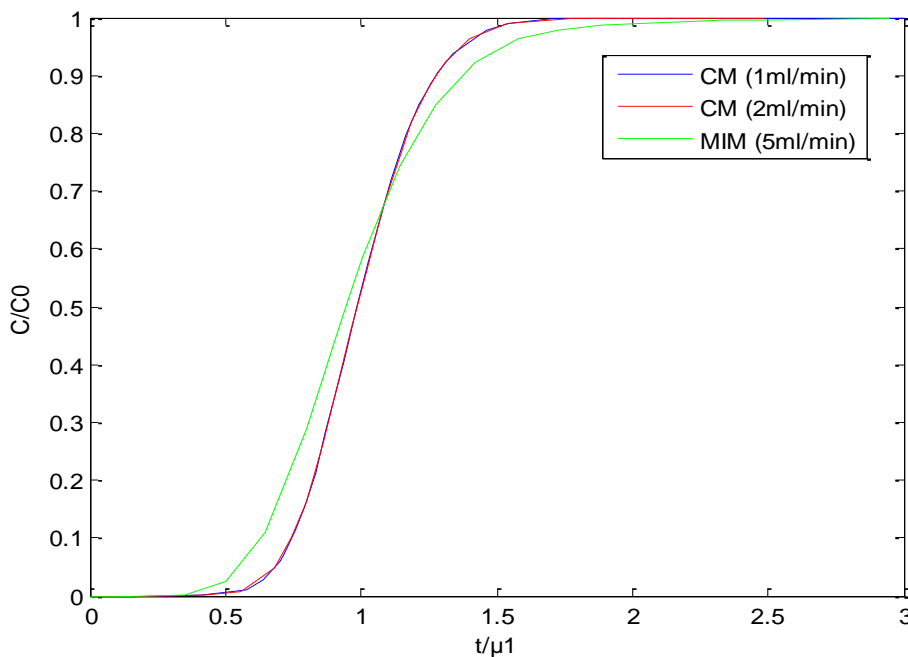


**Fig6:** Effect of the flow rate on BTC.

We note that at the flow rates 1 and 2 ml / min the BTCs are perfectly superimposed, but for the flow rate 5ml/min the BTC present an asymmetry.

Flow rate (ml/min)	1	2	5
R <sup>2</sup> MIM	0.9979	0.9951	0.9992
R <sup>2</sup> CM	0.9989	0.9988	0.9986
$\sigma'^2_{exp}$	0.0456	0.0511	0.1116
$\sigma'^2_{theor\ MIM}$	0.0435	0.0435	0.1036
$\sigma'^2_{theor\ CM}$	0.0435	0.0435	0.0833

**Table 4:** Fitting parameters derived by the CM model and the MIM model.

# International Journal of Innovative Research in Science, Engineering and Technology

(An ISO 3297: 2007 Certified Organization)

Vol. 5, Issue 11, November 2016

According to this table, we note that the experimental BTCs obtained for flow rates 1 and 2 ml/min are represented well by the CM model, while the curve obtained for the flow rate 5ml/min is represented better by MIM model, therefore for the flow rate 5ml/min the immobile phase exists and that explains the shift obtained in the BTC of the flow rate 5ml/min (Fig 6).

## VII. CONCLUSIONS

A new analytical solution was presented for MIM model which takes in the account the PNE to provide a real description of solute transport in porous media. The solution was obtained using the residue theorem to calculate the inverse Laplace transformation of the global function obtained by discrete approach.

The analytical solutions for the CM and MIM models were used to fit experimental BTCs for three values of flow rates, this involved optimization of the parameters of each models. The comparison between the two models at different flow rates show that at a high flow rate (great than 5ml/min) the MIM model tends to fit data better than CM model, so the effect of the flow rate is more important at high value. That can be explained by the Physical nonequilibrium (PNE) which affects the solute transport; this note is in according to the result found by Yan Li Jiang et al [20]. The detection of PNE in soils is commonly achieved by applying MIM model, the presence of the aggregates which trap water in their microporosity, that modifies the flow but also the distribution of the solute in soil, in this case the description of the results is incompatible with the use of the CM model. The use of the MIM model is justified when the breakthrough curve of solute has a strong asymmetry (stiff face going up and face going down trailing). The MIM model can be best to approach the real behavior of solute in the porous medium.

This research examined the effect of the flow rates on the solute transport in porous media, the effects were also reflected in the parameters of the CM and MIM models. An analysis of the model parameters showed that, when the flow rate increased, the immobile fraction and the mass transfer coefficient tended to increase. However, experimental data from other studies showed that the fraction immobile increase with increasing pore water velocity when using curve-fitting procedures [52, 53]. This is consistent with the results of this study. In order to determine the changes of various model parameters under different conditions, they should be verified from several experiments. This form of research should be further advanced to better control conditions.

## REFERENCES

- [1] Birk S, Liedl R, Sauter M. "Karst spring responses examined by process-based modeling". *Ground Water*. Vol. 44, no.6, pp.832–836, 2006.
- [2] Freeze R A and Cherry J A" *Groundwater Englewood Cliffs*", N.J.: Prentice-Hall, 1979.
- [3] Nkedi-Kizza P, Biggar JW, Selim HM, Van Genuchten MTh, and Wierenga PJ. "Equivalence of two conceptual models for describing ion exchange during transport through an aggregated Oxisol". *Water Resour Res*. Vol. 20, pp.1123–1130, 1984.
- [4] Hendrickx JMh and Flury M. "Uniform and preferential flow mechanisms in the vadose zone". In *Conceptual models of flow and transport in the fractured vadose zone*. National Academy Press, Washington, DC pp. 149–187,1984.
- [5] Pot V, Šimůnek J, Benoit P, Coquet Y, Yra A and Martinez-Cordon M J. "Impact of rainfall intensity on the transport of two herbicides in undisturbed grassed filter strip soil cores". *J. Contam. Hydrol*. 81:63–88, 2005.
- [6] Kohne JM, Kohne S and Šimůnek J. "Multi-process herbicide transport in structured soil columns: Experiment and model analysis". *J. Contam. Hydrol*. Vol. 85:pp.1–32, 2006.
- [7] Šimůnek J and Van Genuchten MTh. "Modeling nonequilibrium flow and transport with HYDRUS". *Vadose Zone J. Special Issue "Vadose Zone Modeling"* Vol. 7, pp.782–797, 2008.
- [8] Van Genuchten MTh and Wierenga PJ. "Mass transfer studies in sorbing porous media: Analytical solutions". *Soil Sci. Soc. Am. J*. Vol. 40, no.3, pp. 473–479, 1976.
- [9] Gillham RW, Sudicky EA, Cherry JA and Frind EO. "An advection- diffusion concept for solute transport in heterogeneous-unconsolidated geological deposits". *Water Resour Res*. Vol 20, no. 3, pp. 369–378, 1984.
- [10] Sudicky EA, Gillham RW and Frind EO. "Experimental investigation of solute transport in stratified porous media", 1. The nonreactive case. *Water Resour Res*. Vol. 21, no 7, pp. 1035–1041, 1985.

# International Journal of Innovative Research in Science, Engineering and Technology

(An ISO 3297: 2007 Certified Organization)

Vol. 5, Issue 11, November 2016

- [11] Starr RC, Gillham RW and Sudicky EA. "Experimental investigation of solute transport in stratified porous media", 2. The reactive case. *Water Resour Res.* Vol 21,no7, pp. 1043–1050, 1985.
- [12] Van Duijn CJ and van derZee SEATM. "Solute transport parallel to an interface separating two different porous materials". *Water Resour Res.* Vol 22, no.13, pp. 1779–1789, 1986.
- [13] Liu Gang Si and Bing C. "Analytical modeling of one dimensional diffusion in layered systems with position dependent diffusion coefficients". *Advances in water Resour Res.* Vol. 31, no 2, pp.251–268, 2008.
- [14] Swami D, Sharma PK And Ojha CSP. "Simulation of experimental breakthrough curves using multiprocess non-equilibrium model for reactive solute transport in stratified porous media. *Sadhana*". Vol. 39, no 6, pp. 1425–1446, 2014.
- [15] Ritsema CJ, Dekker LW, Hendrickx JHM, Hamminga W. "Preferential flow mechanism in a water repellent soil". *Water Resour Res.* Vol. 29, pp.2183–2193, 1993.
- [16] de Rooij GH. "Modeling fingered flow of water in soils owing to wetting front instability: a review". *J. Hydrol.* 231–232, pp.277-294, 2000.
- [17] Wang Z, Jury WA, Tuli A, Kilm DJ. Unstable flow during redistribution: controlling factors and practical implications. *Vadose Zone J*; Vol. 3, 549–559, 2004.
- [18] Coats KH and Smith BD. "Dead-end pore volume and dispersion in porous media". *Soc. Pet. Eng. J.* 4, pp. 73–84, 1964.
- [19] Van Genuchten MTh and Wierenga PJ. "Mass transfer studies in sorbing porous media: I. Analytical solutions". *Soil Sci. Soc. Am. J.* Vol. 40, no. 473–480, 1976.
- [20] Jiang Y, Zhou B, Shao M, Wang QJ. "Experimental study on preferential solute transport in Loess Plateau soil". *AJCS.* Vol. 7, no 1, pp.93-98, 2013.
- [21] Van Genuchten MTh, Naveira-Cotta C, Skaggs TH, Raoof A, and Pontedeiro EM. "The Use of Numerical Flow and Transport Models in Environmental Analyses". W.G. Teixeira et al. (eds.), *Application of Soil Physics in Environmental Analyses. Progress in Soil Science.* Springer International Publishing Switzerland, pp 349-376, 2014.
- [22] Šimůnek J, Bradford S. "Vadose zone modeling: introduction and importance". *Vadose Zone J. Special Issue "Vadose Zone Modelling"* Vol. 7, no 2, pp. 581–586, 2008.
- [23] Mallants D, van Genuchten MT, Šimůnek J, Jacques D, Seetharam S. "Leaching of contaminants to groundwater". In: Swartjes FA (ed) *Dealing with contaminated sites; from theory to practical application*, Chapter 18. Springer, Dordrecht. pp 787–850, 2011.
- [24] Jarvis NJ. "The MACRO model (Version 3.1), technical description and sample simulations". *Reports and Dissertations 19.* Department of Soil Science, Swedish University of Agricultural Sciences, Uppsala, Sweden. 51 pp, 1994.
- [25] Šimůnek J, Suarez DL, Šejna M. "The UNSATCHEM software package for simulating one-dimensional variably saturated water flow, heat transport, carbon dioxide production and transport, and multicomponent solute transport with major ion equilibrium and kinetic chemistry". Version 2.0. Research Report No. 141, U.S. Salinity Laboratory, USDA, ARS, Riverside, CA, 186 pp, 1996.
- [26] Zyvoloski GA, Robinson BA, Dash ZV, Trease LL. "Summary of the models and methods for the FEHM application – a finite element heat and mass-transfer code". Los Alamos National Laboratory Rept, 1997.
- [27] Yeh GT, Salvage KM, Gwo JP, Zachara JM, Szecsody JE. "HYDROBIOGEOCHEM: a coupled model of hydrological transport and mixed biochemical kinetic/equilibrium reactions in saturated-unsaturated media", 1998.
- [28] Healy RW. "Simulating water, solute, and heat transport in the subsurface with the VS2DI software package". *Vadose Zone J. Special Issue "Vadose Zone Modelling"* Vol. 7, pp.632–639, 2008.
- [29] Panday S, Huyakorn PS. "MODFLOW SURFACT: a state-of-the-art use of vadose zone flow and transport equations and numerical techniques for environmental evaluations". *Vadose Zone J.* Vol 7, pp. 610–631, 2008.
- [30] White MD, Oostrom M, Rockhold ML, Rosing M. "Scalable modeling of carbon tetrachloride migration at the Hanford site using the STOMP simulator". *Vadose Zone J.* 7:654–666, 2008.
- [31] Van Dam JC, Groenendijk P, Hendriks RFA, Kroes JG. "Advances of modeling water flow in variably saturated soils with SWAP". *Vadose Zone J.* Vol. 7, pp.640–635, 2008.
- [32] Šimůnek J, van Genuchten MT, Sejna M. "Development and applications of the HYDRUS and STANMOD software packages and related codes. *Vadose Zone J. Special Issue "Vadose Zone Modelling"* Vol. 7, no. 2, pp. 587–600, 2008.
- [33] Finsterle S, Doughty C, Kowalsky MB, Moridis GJ, Pan L, et al. (2008) "Advanced vadose zone simulations using TOUGH". *Vadose Zone J.* 7:601–609.
- [34] Neville CJ, Ibaraki M, Sudicky EA. "Solute transport with multiprocess nonequilibrium: a semi-analytical solution approach". *J. Contam. Hydrol.* Vol. 44, pp. 141–159, 2000.
- [35] Semra S. "Dispersion de solutés réactifs en milieu poreux chimiquement hétérogène". Thèse, Génie des Procédés. Nancy, INPL, 2003.
- [36] Leij FJ, Bradford SA. "Combined physical and chemical nonequilibrium transport model: Analytical solution, moments, and application to colloids". *Journal of Contaminant Hydrology.* Vol. 110, pp.87–99, 2009.
- [37] Sardin M. "Modélisation du transport transitoire de solutés en milieux poreux: Les modèles linéaires. Strasbourg. Strasbourg: Sciences Géologiques, Bulletin N°" Vol. 46, pp 197-216, 1993.
- [38] Semra S, Sardin M, Simonnot MO. "A New Mixing-Cell-in-Series Model to Predict Breakthrough Curve in Chemically Heterogeneous Media at Column Scale". *Chemical Product and Process Modeling.* Volume 4, Issue 1, ISSN, 1934-2659, 2009.
- [39] Sardin M et al. "Modeling the nonequilibrium transport of linearly interacting solutes in porous media: A Review". *Water Resources Research.* Vol. 27, N° 9, pp 2287-2307, 1991.
- [40] Stehfest H. "Algorithm 368: numerical inversion of Laplace transforms [D5]". *Communications of the ACM* Vol. 13, no 1, pp. 47-49, 1970.
- [41] Crump KS. "Numerical inversion of Laplace transforms using a Fourier-series approximation". *Journal of the ACM* Vol. 23, no. 1, pp. 89-96, 1976.
- [42] de Hoog FR, Knight JH, Stokes AN "An improved method for numerical inversion of laplace transforms". *SIAM Journal of Scientific and Statistical Computing* Vol. 3, no. 3, pp. 357-366, 1982.

## International Journal of Innovative Research in Science, Engineering and Technology

(An ISO 3297: 2007 Certified Organization)

**Vol. 5, Issue 11, November 2016**

- [43] Moench AF. "Convergent radial dispersion: a note on evaluation of the Laplace transforms". Water Resources Research Vol. 27, no. 12, pp. 3261-3264, 1991.
- [44] Furman A, Neuman SP. "Laplace-transform analytic element solution of transient flow in porous media". Advances in Water Resources Vol. 26 no.12, pp.1229-1237, 2003.
- [45] Gao G, Zhan H, Feng S, Fu B, Huang G, Ma Y. "A new mobile-immobile model for reactive solute transport with scale-dependent dispersion". Water Resources Research Vol. 46, W08533, 2010.
- [46] Gao G, Zhan H, Feng S, Fu B, Huang G. "A mobile-immobile model with an asymptotic scale-dependent dispersion function". Journal of Hydrology. Pp. 424-425, 172-183, 2012.
- [47] Hazewinkel M." Cauchy integral theorem. Encyclopedia of Mathematics", Springer ed, 2001.
- [48] Villiermaux J. "Génie de la réaction chimique: Conception et fonctionnement des réacteurs". Paris, France : TEC&DOC-LAVOISIER, pp.448, 1993
- [49] Coats KH and Smith BD. "Dead-end pore volume and dispersion in porous media". Soc. Pet. Eng. J.Vol.4, pp. 73-84, 1964.
- [50] Chen YM, Abriola LM, Alvarez JJ, Anid PJ, Vogel TM. "Modeling transport and biodegradation of benzene and toluene in sand aquifer material: comparison with experimental measurements". Water Resour. Res. Vol. 28, no.7, pp. 1833-1847, 1992.
- [51] Tevissen E. "Méthodologie d'étude et modélisation du transport de solutés en milieux poreux naturels : application à la migration du chrome dans la nappe alluviale du Drac (Isère)". 1993.
- [52] Li L, Barry DA, Culligan-Hensley PJ, Bajracharya K. "Mass transfer in soils with local stratification of hydraulic conductivity". Water Resour Res. Vol. 30. Pp. 2891-2900, 1994.
- [53] Seyfried MS, Rao PSC. "Solute transport in undisturbed columns of an aggregated tropical soil: Preferential flow effects". Soil Sci Soc Am J. no. 51, pp.1434-1444, 1987.